Observation of offshore wind farm wakes by spaceborne synthetic aperture radar

LI Xiaoming [1, 2], LEHNER Susanne[1]

1. *Key Laboratory of Digital Earth Science, Institute of Remote Sensing and Digital Earth, Chinese Academy of Sciences, Beijing* 100094*, China*;
2. *Laboratory for Regional Oceanography and Numerical Modeling, Qingdao National Laboratory for Marine Science and Technology, Qingdao* 266235*, China*

Abstract: In this paper, studies on offshore wind farm wakes observed by spaceborne SAR (Synthetic Aperture Radar) are reviewed mainly based on our previous research. Particularly, we focus on investigating wind wakes and tidal current wakes observed by spaceborne SAR of TerraSAR-X, Gaofen-3 and Radarsat-2 in high spatial resolution, in two offshores wind farms, i.e. the Alpha Ventus in the North Sea and the one near Donghai bridge in the East China Sea. Representing examples of wind wakes and tidal current wakes observed by SAR in the two farms are presented and compared. A preliminary statistical analysis on morphology of wind feature downstream Alpha Ventus is presented as well. Besides these studies on wind wakes generated by a single offshore wind farm, we show an example of wakes downstream multiple wind farms in the North Sea to demonstrate "cluster" effect of multiple offshore wind farms on sea wind.

Key words: offshore wind farm wakes, synthetic aperture radar

Citation format: Li X M and Lehner S. 2020. Observation of offshore wind farm wakes by spaceborne synthetic aperture radar. Journal of Remote Sensing(Chinese). 24(S1): 110−117

1 INTRODUCTION

With the expansion of global economy, the increasing demand for the fossil fuels leads to serious environmental pollution problems, which poses a great threat to people's health. Wind energy, as a renewable energy, has been abundant transformed to electrical energy, which is regarded as a green energy to meet requirements of both increasing energy consumption and reduction of greenhouse gases emission. Wind farms have been widely constructed in onshore and offshore to obtain wind energy. As surface roughness in the sea is much less than that in the land, offshore wind farms generally are expected to generate more electricity power as mean wind speeds in the sea are higher.

When the wind flows the rotating turbines, wind energy is extracted and converted to electric power. Wind turbulent wake in a spiral shape is formed downstream and it can propagate along axis of turbine for tens of kilometers (Platis *et al.*, 2018), meanwhile it can also laterally expand. The reason that wind turbine wakes drawn great attentions on is they have significant influence on the energy production of the wind farms. Nowadays wind turbines are often placed cluster in order to convert wind energy to electrical energy effectively and economically. Therefore, wake effects of neighboring turbines are important for energy production (Méchali *et al.*, 2006), which should be also taken in account in micro-siting of wind farms (Schneiderhan *et al.*, 2005). A photo taken by a helicopter over the offshore wind farm Horns Rev in the North Sea present spatial patterns of turbulent wakes (Hasager *et al.*, 2013) in near and far fields, as well as their influences on each other. The photo brings strong visual impression of the generated wakes in the huge turbines with diameters of approximately 110 m, close to the wingspan of Airbus-380. Generally, the wind turbine wake is hardly to be observed by eyes. Some remote sensing techniques have been exploited to detect and measure wind turbine wakes.

LIDAR (Light Detection And Ranging) and SODAR (SOund Detection And Ranging) are two advanced remote sensing techniques that have been widely used to detect wind turbine wakes. The two kinds of instruments can determine wind profile by measuring the Doppler shift of returned signals' frequencies of light and sound, respectively. Both are applicable for wake detection and wind profile measurements in onshore and offshore wind farms (Lang and Mckeogh, 2011). Traditionally the SODAR and LIDAR instruments are mounted on fixed platforms, e. g. the transformation station of wind farms or on the ships in the sea (Barthelmie *et al.*, 2003). Along with miniaturization of Doppler wind Lidars, they can be mounted on nacelle of wind turbines. On top of wind turbines, Lidars can perform measurements over conical surface by varying the azimuthal angle, thus multiple wind turbine wakes downstream are possible to be detected (Iungo *et al.*, 2013).

As wind turbine wakes can extend up to tens of kilometers, they also present highly spatial variations in near and far field. Synthetic Aperture Radar, as an active remote sensing instrument, also draws great attention on using it for detecting and measuring

Received: 2019-10-21; **Accepted:** 2020-04-16
Foundation: National Natural Science Foundation of China (No.41471309)
First author biography: LI Xiaoming (1979—), male, full research professor, his research interests is SAR oceanography. E-mail: lixm@radi.ac.cn

offshore wind turbine wakes. However, the way that SAR used to detect offshore wind turbine wake is different from that of Sodar or Lidar. SAR cannot detect directly offshore wind turbine wake, whereas detect sea surface roughness changed by the turbulent wakes. SAR images sea surface primarily following the wide known Bragg scattering mechanism, i.e. radar microwaves are in resonance with sea surface waves of similar scale. As mentioned in the beginning of introduction, the generated wind turbulence not only propagate longitudinally but also expand laterally. Therefore, when the turbulent wakes "touch" the sea surface, it is possible that the sea surface roughness is modulated, and the wakes are consequently "imaged" by SAR. For the first time an airborne SAR was used to map the turbine wake in the offshore wind farm Horns Rev, North Sea (Christiansen & Hasager, 2006), meanwhile the ERS-2/SAR images with spatial resolution of 25 m were also acquired in the experiment. Based on the SAR-derived sea surface wind speed maps, the wake length, width and VD (Velocity Deficit) are investigated. Following the experiments, a more detailed study on wind turbine wakes effect in Horns Rev was conducted based on multiple ERS-2/SAR and ENVISAT/ASAR images (Christiansen & Hasager, 2005), in which the VD was specifically investigated under different weather situations.

One of the most distinguished features of the modern spaceborne SAR, e.g., TerraSAR-X (TS-X), Gaofen-3 (GF-3), Radarsat-2 (R2), compared with the previous SAR sensors is high spatial resolution, up to one meter. This provides us a unique opportunity to study offshore wind farm wakes in multi-scale. Based on these spaceborne SAR images with high spatial resolution, we have found many interesting cases showing various characters of offshore wind farm wakes (Li & Lehner, 2013; Li *et al.*, 2014; Djath *et al.*, 2018). In this paper, we present a review of studies on offshore wind farm wakes using spaceborne SAR data in high spatial resolution. The paper is organized as follows. In Section 2, a few examples taken over the German offshore wind farm Alpha Ventus and the Chinese Donghai bridge offshore wind farms are presented, which show two types of wakes frequently observed in offshore wind farms, i.e. the wind wake and tidal current wake. Then, we focus on statistical analysis of wind wakes observed in Alpha Ventus based on multiple SAR images, which is presented in Section 3. Different from wakes observed in a single offshore wind farm, in Section 4, we present an example showing wind wakes in multiple offshore wind farms in the North Sea. Summary and outlook are given in the last Section.

2 WIND WAKES AND TIDAL CURRENT WAKES OBSERVED IN OFFSHORE WIND FARMS BY SAR

In our previous study (Li & Lehner, 2013), two TS-X images in Stripmap mode acquired over the offshore wind farm Alpha Ventus in the North Sea, the first one in Germany, were analyzed in detail. The TS-X Stripmap mode data have a spatial resolution of 3 meters in both azimuth and range directions. Thanks to capability of imaging sea surface high spatial resolution, the two cases show more clear wind wake features downstream Alpha Ventus than ever before, not only in near and far fields, but also within the wind farm. Fig.1 (a) and (b) are the two TS-X images acquired over Alpha Ventus, and their corresponding sea surface wind speed maps are shown in Fig. 2(a) and (b).

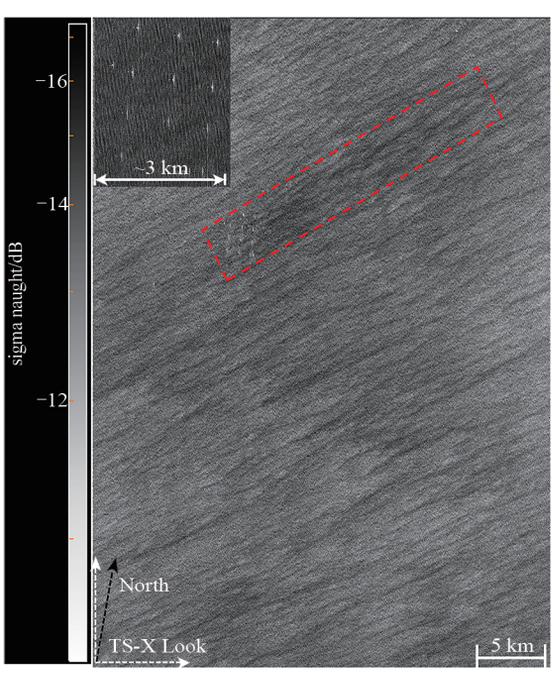

(a) A TS−X image acquired on Aug7, 2011

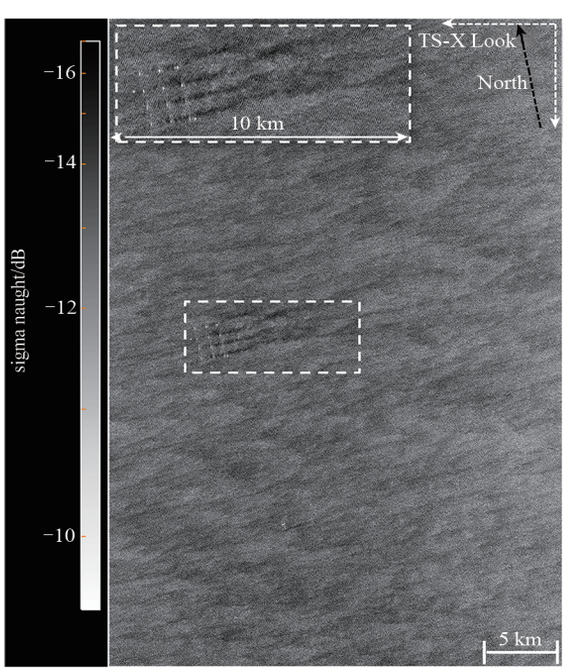

(b) A TS−X image acquired on Aug23, 2012

Fig.1 Two TS−X Stripmap images acquired over the offshore wind farm Alpha Ventus showing distinct wind wakes. In (a), the upper−left overlaid sub−image shows offshore wind turbines of Alpha Ventus; in (b), the overlaid sub−image shows the offshore wind farm and wakes downstream.

Although the both cases show clear wind wakes downstream the offshore wind farm, they have quite different spatial variations. In the case 1 (Aug.7, 2011), the wake length is approximately 18 km, which is about 4 km longer than that in the case 2 (Aug.23, 2012).

Moreover, case 1 has wider wake than that of the case 2, which is particularly evident in the sea surface wind map shown in Fig. 2. The most interesting point of the two cases is the phenomena of wake merging which was observed by first time in high spatial resolution SAR image. In case 2, a quadruple wake pattern (seeing the enlarged sub-image shown in Fig. 1(b)) is clearly presented in the TS-X image and these wakes did not merge completely till 70*D* (diameter of the wind turbine in Alpha Ventus, 116 m) away from the first column of the turbines. However, in the first case, it seems that a wide wake was immediately formed in the near wake region and it extended as one wake till around 18 km downstream of Alpha Ventus. Our explanation on this discrepancy is the incoming wind direction of the two cases was different. In the second case, the wind direction at hub height was 254º (refer to Fig.2(b)), which is nearly parallel to the rows of wind turbines, therefore, the wakes formed in each row may present their original forms for some distances. However, the wind direction in the first case was 225º, meaning the wind was blowing across the offshore wind farm. Thus, wakes may merge quickly under the external wind forces.

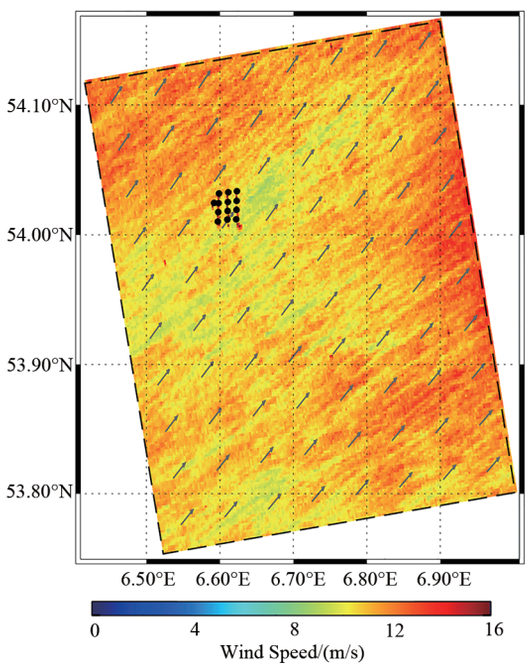

(a) Retrieved sea surface wind for the TS-X image shown in Fig.1(a)

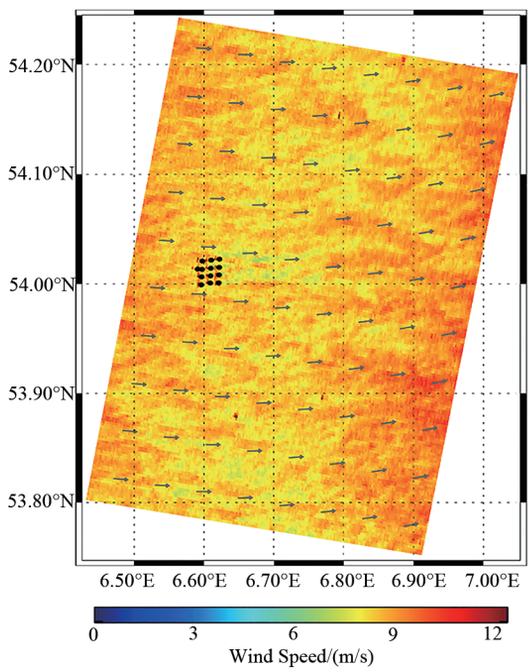

(b) Retrieved sea surface wind for the TS-X image shown in Fig.1(b)

Fig.2 The retrieved sea surface wind maps using the X-band Geophysical Model Function (GMF) XMOD2 (Li & Lehner, 2014) for the two TS-X image shown in Fig.1

In case 2, we can observe that the sea surface backscatter in the area between the second and third columns of the turbines is lower than that in the area between the first and second columns, which indicates that wakes generated upstream arrived at the sea surface after it passed the second column and therefore changed the sea surface roughness. Because of the high spatial resolution of TS-X data, one can identify the wake pattern inside the offshore wind farm, which had never been reported elsewhere to our knowledge.

The two cases show quite different spatial variations of wind wakes in the offshore wind farm Alpha Ventus. Based on detailed analysis presented in Li and Lehner (2013), we believe that these different characters of the wind wakes are significantly related with weather situations, particularly with atmospheric stability and incoming air flow characteristics, such as wind speed, wind direction and turbulence intensity. Nevertheless, these studies reveal that the high spatial resolution SAR images can contribute significantly to studies of offshore wind wakes.

Following the idea of studying wind wakes in the offshore wind farm Alpha Ventus using high spatial resolution SAR data, we also conducted similar studies in the Chinese offshore wind farm. However, we found some quite different wake patterns.

We have acquired numbers of SAR images in X-band and C-band over the Donghai bridge offshore wind farm in the southeast of Changjiang river estuary. Our first impression of seeing the TS-X image shown in Fig.3 was that the "wind wakes" were such distinct over there. However, detailed analysis based on numerical simulations and multiple satellite observations suggests these wakes should be interpreted as tidal current wakes instead of wind wakes, which are generated by interaction between tidal currents and the piles of each offshore wind turbine (Li *et al.*, 2014). A GF-3 FSI image with spatial resolution of 5 m was acquired in 2017, in which we can see that in the west of the bridge, the other wind farm also has been constructed, while tidal current wakes are visible downstream of both wind farms located two sides of the bridge (Li *et al.*, 2018). These wakes are completely different from those we observe in the offshore wind farm Alpha Ventus.

The formation of these tidal current wakes in the Donghai bridge offshore wind farm should at least attribute two reasons. On the one hand, the wind farm locates in the mouth of the funnel-shaped Hangzhou bay where the tidal current is strong, with an observed maximum tidal velocity approaching 5 m/s. Moreover, the tidal current presents an alternating feature; namely, it flows from east to west during flood and reverses during ebb. On the other hand, the piles of the wind turbines at the Donghai Bridge offshore wind farm have a rather specific structure, i. e. so-called "High-Rise pile cap" structure, which is against the soft seabed and the possible shift caused by tide. A remarkable feature of the foundation is the large concrete cap on top of monopile (referring to the

photo in the left panel of Fig. 5). These concrete caps are regular cylinders and have a diameter of 15 m. The strong tidal current has an interaction (seeing the visible wakes in the field photo shown in Fig. 5) with these cylindrical piles and induces water turbulence, which damps the surface Bragg waves, and therefore modulates the sea surface roughness and consequently is imaged by SAR as wakes downstream.

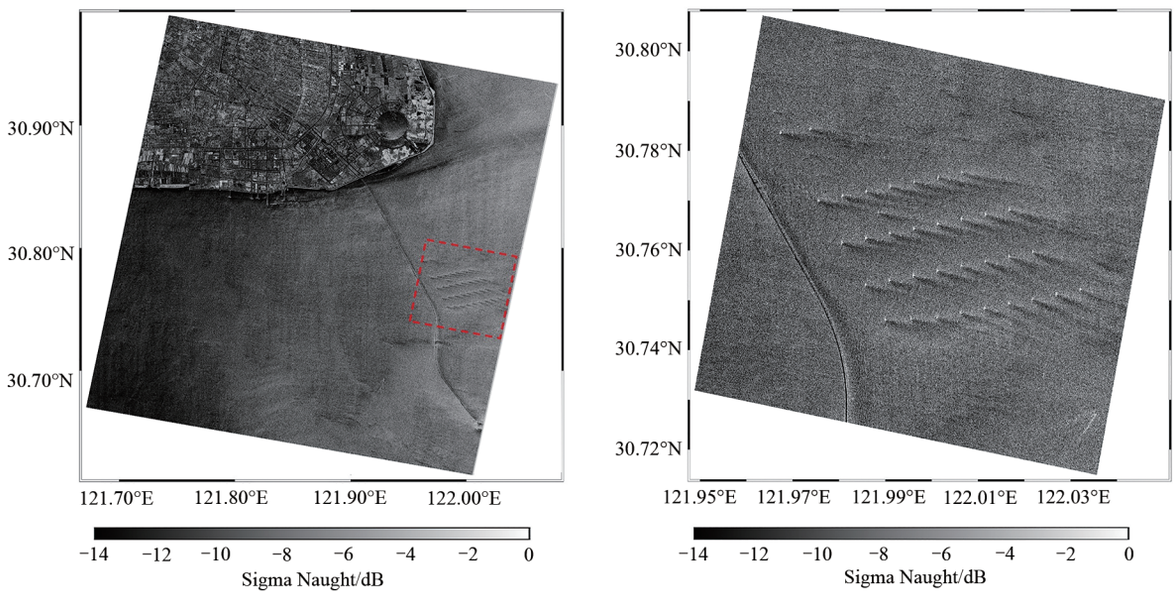

Fig.3 A TS−X Stripmap image in VV polarization acquired on Feb. 8, 2011 over the China Donghai bridge offshore wind farm in the East China Sea and the subscene (right panel) shows distinct tidal current wake downstream each wind turbine.

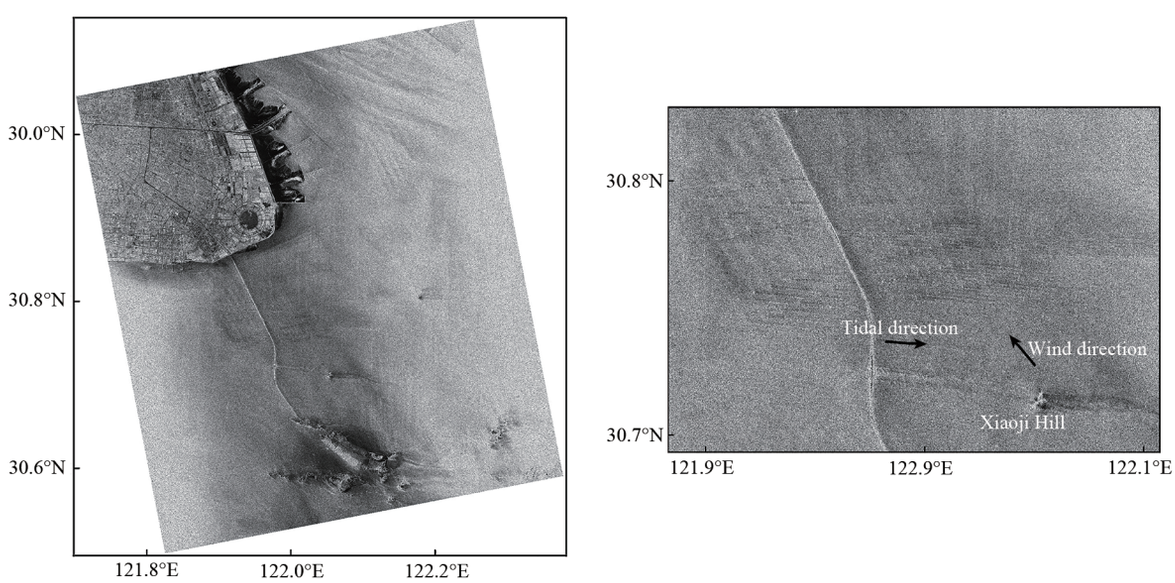

Fig.4 A GF−3 Fine Stripmap Image (FSI) in HH polarization acquired on Feb. 15, 2017 over the eastern Hangzhou Bay and Changjiang River estuary. Right panel is the sub−image over the Donghai bridge offshore wind farm showing distinct tidal current wake patterns.

However, when these tidal current wakes are visible in SAR images, it does not mean that wind wakes are not formed. Fig. 6 shows a Radarsat-2 image acquired in the Donghai bridge offshore wind farm. The sea surface wind was northwesterly, whereas the tidal current flew southeasterly. Again, it presents distinct tidal current wake downstream each wind turbine, as seen in the enlarged sub-scene in the lower-left panel of the figure. However, it is hardly to see any wind wakes in the offshore wind farm.

A synchronized experiment on wake detection by Lidar was carried out in the offshore wind farm. The Lidar instrument was setup on the bridge, which has a height of 30 m above sea surface face. The Lidar was operating in the inclined PPI (Plan Position Indicator) mode with inner cone angle of 120°. During the measurement, the Lidar was fixed at an elevation angle of 2°, meaning it nearly scanned the air at the same height of the bridge. The Lidar measurement of wind profile at 9:45 UTC, at the same time as the Radarsat-2 acquisition, presents a clear offshore wind wake with length of approximately 500 m, at the height of 30 m above sea surface, as shown in Fig.7.

(a) The pile/foundation of a wind turbine

(b) The tidal current wake (clear visible smoothed sea surface) formed downstream of a wind turbine

Fig.5 A photo taken over the Donghai bridge offshore wind farm

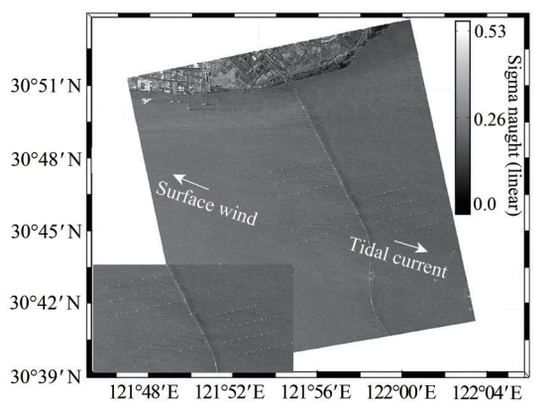

Fig.6 A Radarsat-2 image acquired at 9:45 UTC on May 24, 2016 over the Donghai bridge offshore wind farm. The enlarged sub-image in the lower left panel shows the tidal current wakes

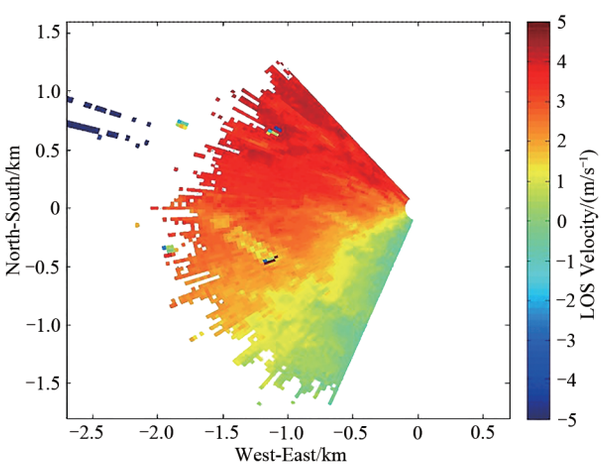

Fig.7 Lidar measurement of wind speed in the orientation of LOS (light of sight) at 9:45 UTC on May 24, 2016. A wind wake at the height of approximately 30 above the sea surface was detected by the Lidar in the orientation of southeast to northwest

This is a convincing example demonstrating the observed dark patterns in high resolution SAR images are tidal current wakes instead of wind wakes. However, the interesting point is why the wind wakes were detected by Lidar whereas they were not imaged by spaceborne SAR. Note that the Lidar measured the wind speed at the height of 30 m above sea surface, while SAR images the sea surface. Therefore, our deduction is that the wakes generated at the hub height was too weak to change the sea surface roughness, resulting in absence of wind wakes in the SAR imagery.

Comparing the wind wakes with tidal current wakes in the offshore wind farms presented above, we can find that they show some discrepancies. The most distinct one is that the tidal current wakes have smaller spatial scales that those of the wind wakes. While the wind wakes often have a length greater than several kilometers (even up to tens of kilometers), the tidal current wakes generally have a length less than a few kilometers. Second is that the wind wakes in the offshore wind farms show more spatial variations, e.g., they often appear wake meandering. The high spatial resolution capability of spaceborne SAR allows us to identify distinct tidal current wakes induced by man-made objects in shallow water. We note that these distinct wind farm turbulent wakes have also been identified in the North Sea offshore wind farm parks (Vanhellemont & Ruddick, 2014). The promotion of clean offshore wind energy must not neglect the changes in local hydrodynamics caused by wind farms and possible associated environmental issues (Grashorn & Stanev, 2016).

3 STATISTICAL ANALYSIS OF WIND WAKES OBSERVED IN ALPHA VENTUS BY SAR

Above we presented a few examples of typical wakes observed by spaceborne SAR in high spatial resolution over the offshore wind farms in both Germany and China. Alpha Ventus has been operating for a few years and some TS-X and TD-X SAR images have been acquired over the offshore wind farm. In this section, we attempt to present a statistical analysis on the wind wake patterns observed in Alpha Ventus.

92 TS-X and TD-X images in ScanSAR, Stripmap and Spotlight modes, while all in VV polarization were collected. Among the SAR images, more than half (56.5%) of cases do not show any visible features downstream the offshore wind farm Alpha Ventus. Therefore, it seems common to observe nothing different from ambient sea surface in SAR images downstream Alpha Ventus. Note that wind turbines have a cut-in speed (3.5 m/s for Alpha Ventus). When the Inflow velocity is higher than that, the blades will rotate normally. After referring to the in-situ wind speed at 90 m height of FINO1 (close to the hub height of 100 m), approximately 20% of the cases are below the cut-in speed, indicating that the turbines are out of operation. On the other hand, even the wind speeds are higher than the cut-in speed, we cannot exclude the possibility that Alpha Ventus was not in operation due to kinds of reasons, e.g., under examination. On the other hand, as shown in the Lidar-SAR experiment on detection wind wakes in the China Donghai bridge offshore wind farm, one can find that even wind wakes are generated, which are not ensured to be detected by SAR imaging sea surface instead of detecting wakes directly.

28 images show clear wind wake feature, while 12 cases show the so-called "jet" feature. Two examples of the wind wake and wind jet observed in Alpha Ventus are shown in Fig.8 (a) and (b), respectively. As analyzed of some typical wind wakes in Alpha Ventus, it is easy to understand such dark patterns shown in Fig.8(a). However, appearance of these wind jet features makes us confused. As it is generally understood, wind energy is converted to electrical power when the air passes through the turbines and therefore wind speed is reduced. However, the jet features presented in SAR images indicate that wind speed increases, which is contrary to general circumstances. Djath *et al.* (2018) proposed a semi-empirical model to explain the increased radar cross section downstream Alpha Ventus observed in SAR images. They attribute this effect to the increased downward momentum flux. However, we think the other possibility is that the turbines (as well as their blades) behav-

ior like obstacles which speed up the airflow downstream, i.e. the "blockage" effect. The reason is that we found other cases showing similar jet features downstream in both offshore wind turbines and offshore platforms (referring to Fig. 9), which show very similar wind jets effect downstream, while the platforms are typical high and wide structures as obstacles in the sea.

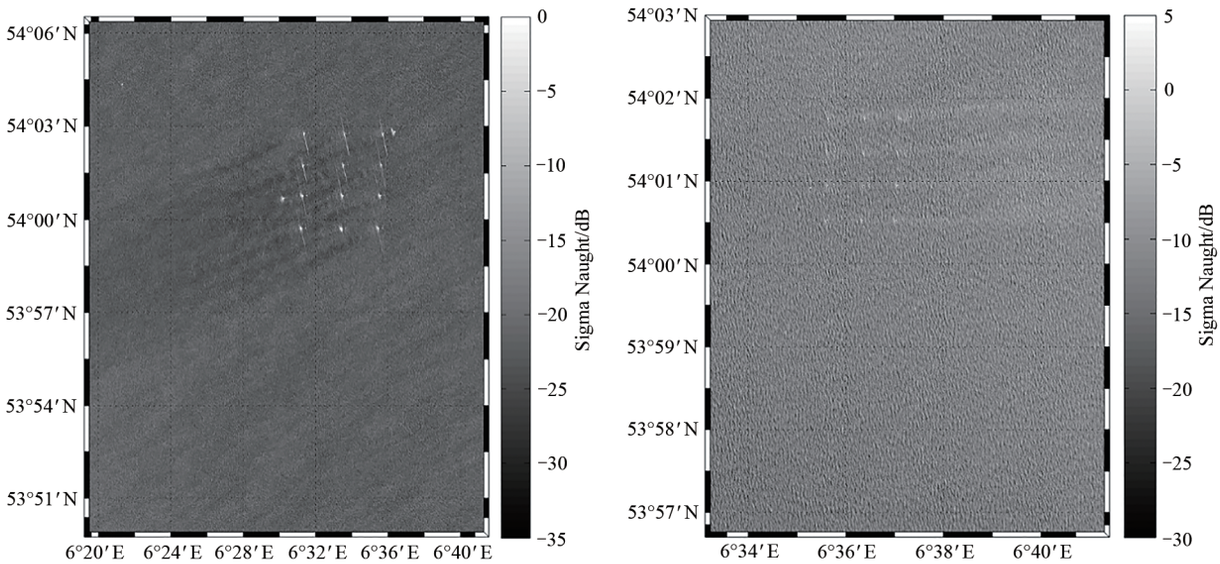

(a) A TS-X image acquired on Dec.11, 2014 (b) A TS-X image acquired on Feb.23, 2012

Fig.8 Two TS-X Stripmap images acquired over Alpha Vetus showing different wind patterns downstream the offshore wind farm.

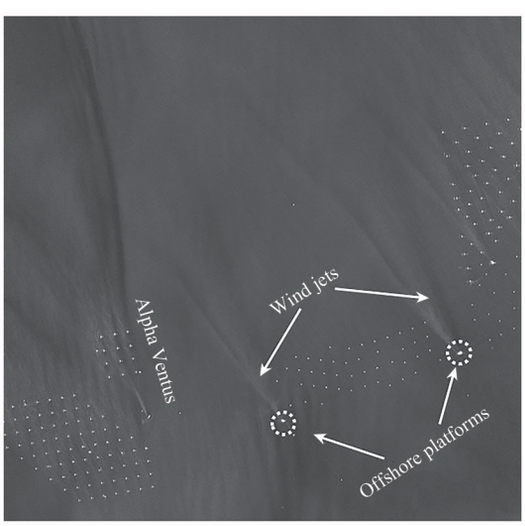

Fig. 9 The quicklook of a TS-X Stripmap image (5:51 UTC, Apr 4, 2016) acquired over several offshore platforms in the North Sea showing distinct wind jet features not only downstream wind farms, but also downstream offshore platforms.

Interestingly is that all the 12 SAR images of wind jets do not show visible wind streaks, for instance, the case shown in Fig. 9. We found that atmosphere stability plays a crucial role in the emergence of wind streaks in SAR images (Zhao *et al.*, 2016). It is found that approximately two thirds of the wind streaks cases occur under unstable atmospheric conditions. Therefore, we can deduce that stable atmosphere might be dominant in the non-wind streaks cases. Unfortunately, in-situ measurements in FiNO1 only were available in 4 cases of the 12 wind jet cases which allows us to calculate atmospheric stability. The result is that the atmosphere was stable in the four cases. Although limited cases were analyzed, it still suggests that atmosphere stability certainly has close relation with the appearance of wind jets downstream of offshore wind farm observed by SAR.

4 WIND WAKES OF MULTIPLE OFFSHORE WIND FARMS OBSERVED BY SAR

The previous sections mainly deal with wakes observed downstream a single wind farm, a very interesting case is presented below showing that downstream wind farms are fully covered by turbine wakes generated by the wind farm upstream, in the vicinity where the Alpha Ventus locates. The case draws our great interests on as influences of wakes generated upstream on the neighboring wind farms have been rarely investigated. So far, it seems that only spaceborne remote sensing data with high spatial resolution can map such kind of phenomena in large scale beyond dozens of kilometers.

Fig. 10 shows a GF-3 FSI image acquired over a few offshore wind farms including Kiffgat, Brokum Riffgrung, Alpha Ventus, Trinael, Innogy Nordsee and Global Tech, in the North Sea. This is a promising SAR image in high spatial resolution (5 m) showing wind wakes generated by multiple wind farms. The Innogy Nordsee wind farm is still under construction, while the visible wind wakes downstream the other four wind farms suggest they were in operation. The most distinguished area is in the vicinity of Brokum Riffgrung, Alpha Ventus and Trianel wind farms.

The wind farms of Alpha Ventus and Trianel locate north of the wind farm Brokum Riffgrung. In this case, the sea surface wind blows from south to north, which makes that Alpha Ventus and Trianel locate downstream Brokum Riffgrung. The NRCS (Normalized Radar Cross Section) in the vicinity is darker than other areas imaged by the SAR, which may suggest the "cluster" effect of multiple wakes of the three offshore wind farms. Alpha Ventus was completely covered by wakes generated by Brokum Riffgrung, while part of

the Trianel was not. Therefore, we chose four transects (dashed lines shown in Fig.10(b)) to analyze variation of sea surface wind speed inside and outside of the wind farms, as shown in Fig. 11. The sea surface wind speed was retrieved using the C-band GMF (Geophysical Model Function) CMOD5. N. The sea surface wind direction used in the retrieval is from the ECMWF-Interim reanalysis wind data.

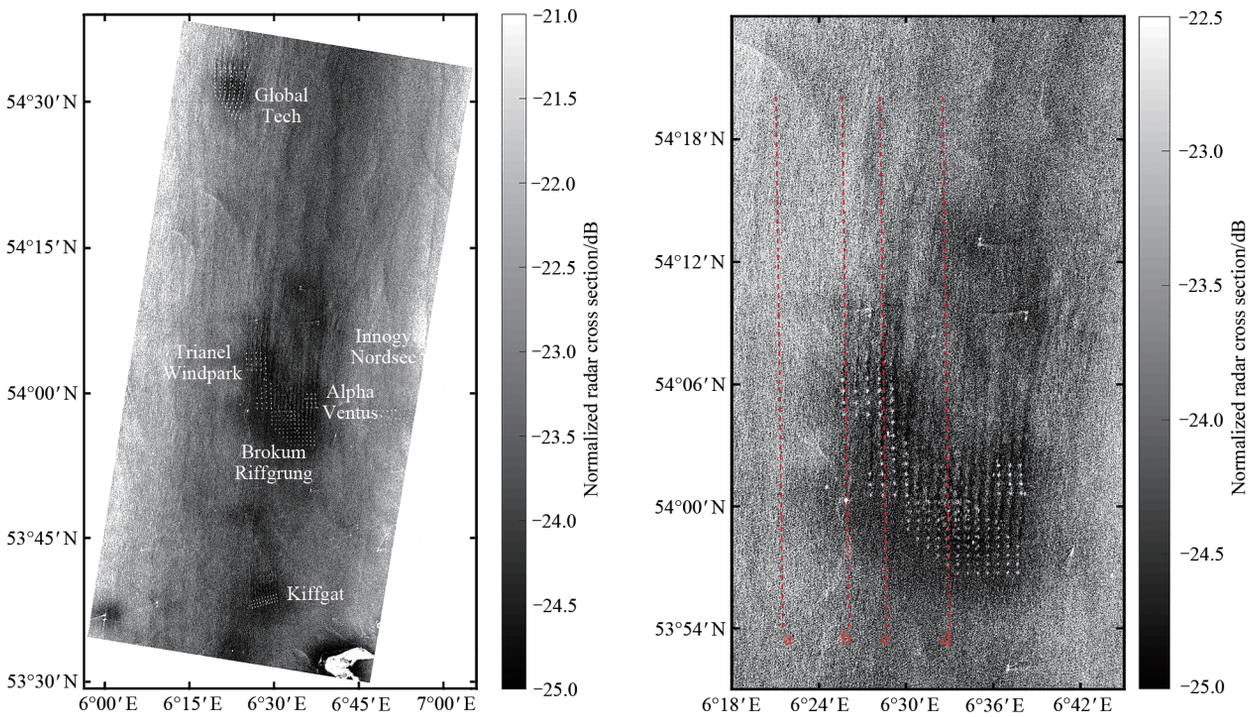

(a) The GF-3 FSI image acquired on Mar. 8, 2017 over multiple wind farms in the North Sea

(b) A sub-image of the GF-3 image covering three wind farms of Trianel, Alpha Ventus and Broum Riffgrung

Fig. 10 A GF-3 FSI image acquired over multiple offshore wind farms in the North Sea

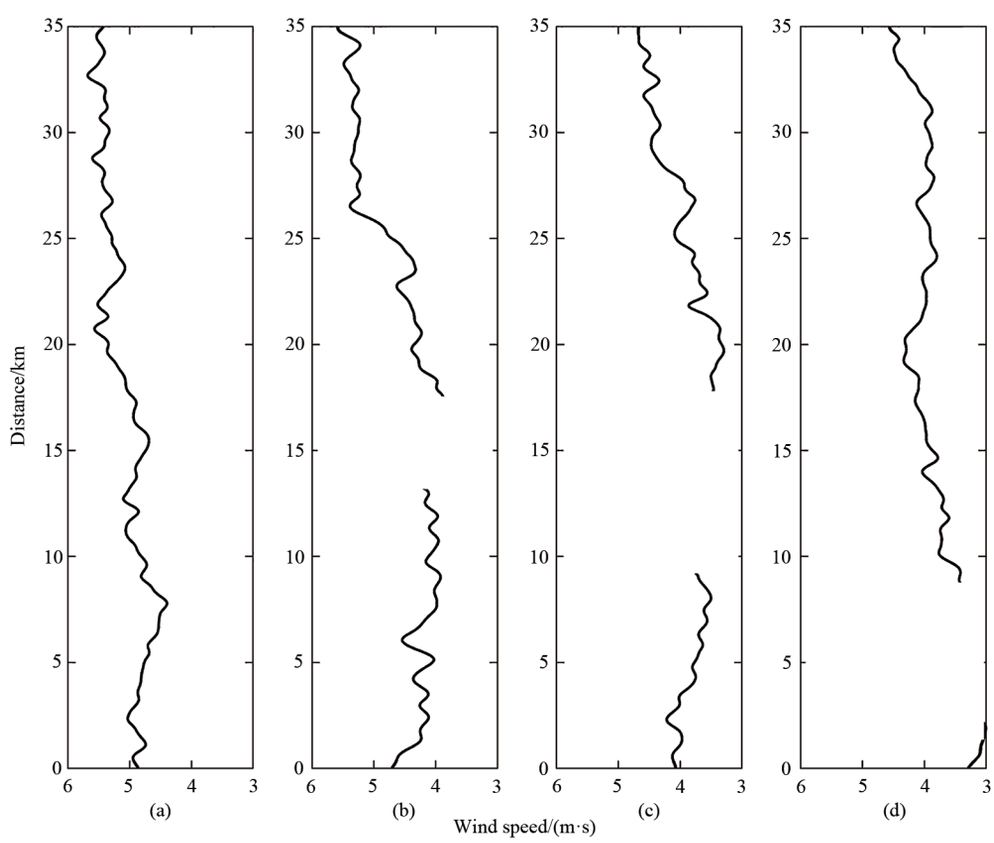

Fig. 11 Variation of sea surface wind speed in the four transects a, b, c and d shown in Fig.10 (b)

The transect a somehow presents wind situation in the ambient sea, which shows the upstream sea surface wind speed was approximately 5 m/s. Transect b is through the most western column wind turbines of Trianel. Variation of sea surface wind speed in the transect b suggests that wind speed recovered to approximately 5 m/s at around 7.5 km downstream; namely, the wake length is around 7.5 km. However, wind speed in transect c reaches to about 4.5 m/s at around 17.5 km downstream. This transect exactly covers upstream and downstream wind farms, therefore, the fact of longer wake length of transect c than that of transect b clearly reveals the influence of wind farm upstream on downstream.

The other interesting point is the "cluster" of multiple offshore wind farms seems to affect wind upstream as well. The SAR image shows there is a dark area upstream the three wind farms. From the transect a to d, the sea surface wind speed decreased from 5.0 m/s to 3.3. m/s further proves this effect.

5 SUMMARY AND OUTLOOK

In this paper, wake patterns in offshore wind farms observed by spaceborne SAR with high spatial resolution are investigated. North Sea is the most active area of building up offshore wind farms in the world, where dozens of wind parks have been in operation. Wakes have significant impacts not only on energy production, but also on natural environment. The modern spaceborne SAR sensors have higher spatial resolution in the scale of a few meters. Therefore, this provides unique advantage of observing these wakes' footprints on the sea surface and further to study wake characters within the wind farms, in near and far fields.

Numbers of spaceborne SAR images acquired over the wind farms in the North Sea, e.g., Alpha Ventus, have shown these wind turbine wakes exhibit highly variable characters, which might be more complicated than what we think. On the other hand, turbine wakes are three-dimensional features, while SAR only images the sea surface in two-dimension. Therefore, comprehensive experiments should be designed, e. g., combining with Lidar measurements, to better interpret turbine wake features observed in SAR images.

Compared with wind turbine wakes that are widely observed by SAR in the North Sea offshore wind farms, few SAR images present wind turbine wakes in the China offshore wind farms. Instead, the tidal current wake features are very distinct. This is because many offshore wind farms are built up in shallow water in China, while tidal currents are rather significant in coastal zones. Their interactions with piles of wind turbines are significant, implying local hydrodynamics might be changed significantly by these man-made objects.

There are few issues that should be investigated in the future regarding on detecting wind turbine wakes using spaceborne SAR. There are many cases that we do not observe wind turbine wakes in SAR images. On one hand, we should communicate with offshore wind farm enterprises to exclude the cases that the wind farms are not in operation, not only because low wind speeds. Second, conducting numerical simulations to verify to what extent that the changed sea surface roughness by the wake turbulence can lead to footprints of these wakes imaged by SAR. The observed increased radar backscatter features downstream wind farms certainly remain further investigation. Previously, we mainly focus on wake effects downstream of wind farms, however, while more wind farms tend to be built up in cluster, they have formed a huge obstacle in the air, and it seems that the airflow in the near upstream is also affected.

Along with more spaceborne SAR in orbits, we believe that temporal intervals of SAR acquisitions will be significantly reduced, and this can contribute to continuous observation of wind wakes instead of only single cases.

REFERENCES

Barthelmie R J, Folkerts L, Ormel F T, Sanderhoff P, Eecen P J, Stobbe O and Nielsen N M 2003. Offshore wind turbine wakes measured by SODAR. Journal of Atmospheric and Oceanic Technology, 20 (4): 466-477

Christiansen M B and Hasager C B 2005. Wake effects of large offshore wind farms identified from satellite SAR. Remote Sensing of Environment 98(2-3): 251-268

Christiansen M B and Hasager C B 2006. Using airborne and satellite SAR for wake mapping offshore. Wind Energy, 9(5): 437-455.

Djath B, Schulz-Stellenfleth J and Cañadillas B 2018. Impact of atmospheric stability on X-band and C-band synthetic aperture radar imagery of offshore windpark wakes. Journal of Renewable Sustainable Energy, 10, 043301 (2018)

S and StanevGrashorn, E V 2016. Kármán vortex and turbulent wake generation by wind park piles. Ocean Dynamics, 66(12): 1543-1557

Hasager C B, Nygaard N G, Volker P J H, Karagali I, Andersen S J, Badger J 2017. Wind farm wake: the 2016 Horns Rev Photo Case. Energies, 10(317):696-716

Iungo G V, Wu Y and Porté-Agel F 2013. Field measurements of wind turbine wakes with Lidars. Journal of Atmospheric and Oceanic Technology, 30:274-287

Lang S and mckeogh E 2011. LIDAR and SODAR measurements of wind speed and direction in upland terrain for wind energy purposes. Remote Sensing, 3(9): 1871-1901

Li X-M and Lehner S 2013. Observation of terrasar-X for studies on offshore wind turbine wake in near and far Fields. IEEE Journal of Selected Topics in Applied Earth Observations and Remote Sensing, 6(3): 1757-1768

Li X-M and Lehner S 2014. Algorithm for sea surface wind retrieval from terrasar-X and tandem-X data. IEEE Transactions on Geoscience and Remote Sensing, 52(5):2928-2939

Li X-M, Chi L, Chen X, Ren Y and Lehner S 2014. SAR observation and numerical modeling of tidal current wakes at the East China Sea offshore wind farm. Journal of Geophysical Research: Oceans, 119: 4958-4971

Li X-M, Zhang T, Huang B and Jia T 2018. Capabilities of Chinese Gaofen-3 synthetic aperture radar in selected topics for coastal and ocean observations. Remote Sensing, 10(12):1-22

Méchali M, Barthelmie R J, Frandsen S, Jensen L G and Réthoré P-E 2006. Wake effects at Horns Rev and their influence on energy production. In Proceedings of the European Wind Energy Conference and Exhibition 2006 (EWEC 2006), Athens, Greece, 1-10

Platis A, Siedersleben S K, Bange J, Lampert A, Bärfuss K, Hankers R, Cañadillas B, Foreman R, Schulz-Stellenfleth J, Djath B, Neumann Th and Stefan E 2018. First in situ evidence of wakes in the far field behind offshore wind farms. Scientific Reports, 8:2163

Schneiderhan T, Lehner S, Schulz-Stellenfleth J and Horstmann J 2005. Comparison of offshore wind park sites using SAR wind measurement techniques. Meteorology Applications, 12(2): 101- 110

Vanhellemont, and Ruddick KQ 2014. Turbid wakes associated with offshore wind turbines observed with Landsat 8. Remote Sensing of Environment, 145:105 – 115

Zhao Y, Li X-M and Sha J 2016. Sea surface wind streaks in spaceborne synthetic aperture radar imagery. Journal of Geophysical Research: Oceans, 121: 6731-6741